

# Monte Carlo Simulation of the 2D Ising model

Emanuel Schmidt, F100044

April 6, 2011

## 1 Introduction

Monte Carlo methods are a powerful tool to solve problems numerically which are difficult to be handled analytically. Nevertheless, these methods are applied to one of the best studied models in statistical physics in the following: The Ising model, which was invented by Wilhelm Lenz and investigated by his student Ernst Ising in the 1920ies. In particular, the two-dimensional case with interactions between next neighbours only is considered. Setting the coupling constant to 1, the Hamiltonian used here reads

$$H = - \sum_{\langle ij \rangle} \sigma_i \sigma_j$$

where  $\langle ij \rangle$  denotes all neighbouring pairs and  $\sigma_i \in \{1, -1\}$  characterizes the spins on the lattice. This model exhibits a second order phase transition, and Onsager found an exact solution in 1944.

In this report, implementations of the Ising model by means of two different algorithms are discussed. First, the single-spin flip Metropolis algorithm is used to investigate thermalization processes and auto-correlation times as well as for making a first measurement of the magnetization and susceptibility in the critical region. Next, measurements at different lattice sizes are performed by means of the Wolff algorithm. Using these results, values for the critical temperature  $T_C$  and the critical exponents  $\gamma, \nu$  are determined which can be compared to the known theoretical values. The implementation was done in C under Scientific Linux and Originlab OriginPro was used for evaluating and plotting the data.

A necessary condition for a Monte Carlo algorithm based on a Markov process is *ergodicity*, which means that the time average is equal to the average over multiple systems. Equivalently, any state of the system can be reached from any other state. This turns out to be obvious for both algorithms, except for the very special case  $T = 0$  we are not interested in. To ensure that the algorithm works properly, the additional condition of *detailed balance* is sufficient, that is,

$$p_A T(A \rightarrow B) A(A \rightarrow B) = p_B T(B \rightarrow A) A(B \rightarrow A) \quad \forall A, B$$

where  $T(A \rightarrow B)$  is the probability to propose moving from  $A$  to  $B$  and  $A(A \rightarrow B)$  is the probability to accept a move from  $A$  to  $B$ , and accordingly for  $B \rightarrow A$ . The probabilities  $p_A$  and  $p_B$  have to satisfy

$$\frac{p_A}{p_B} = \frac{\frac{1}{Z} e^{-\beta E_A}}{\frac{1}{Z} e^{-\beta E_B}} = e^{-\beta \Delta E} \quad \text{where} \quad \Delta E = E_A - E_B$$

in order to sample the Boltzman distribution. From this latter condition, constraints on the algorithms can be derived.

## 2 The Metropolis algorithm

The single-spin flip Metropolis algorithm randomly chooses a spin from an  $L \times L$  lattice and determines the energy difference to the state where this spin is flipped. In order to get detailed balance, the probability of accepting the new configuration is set to

$$A(A \rightarrow B) = \text{Min} \left\{ 1, e^{+\beta(E_A - E_B)} \right\}.$$

This procedure is repeated for a predetermined number of time steps, where it is convenient to count the time  $t$  in time steps per lattice site. To avoid treating the boundaries of the lattice differently, periodic boundary conditions are imposed. For all simulations in this section, a  $40 \times 40$  lattice was used.

## 2.1 Thermalization process

One may choose from two initial states of the lattice, either equally distributed spins corresponding to an inverse temperature of  $\beta = 0$  or all spins aligned in the same direction corresponding to  $\beta = \infty$ . It is first determined how long the algorithm takes to reach an equilibrium at a given inverse temperature  $\beta$ , starting from these initial states.

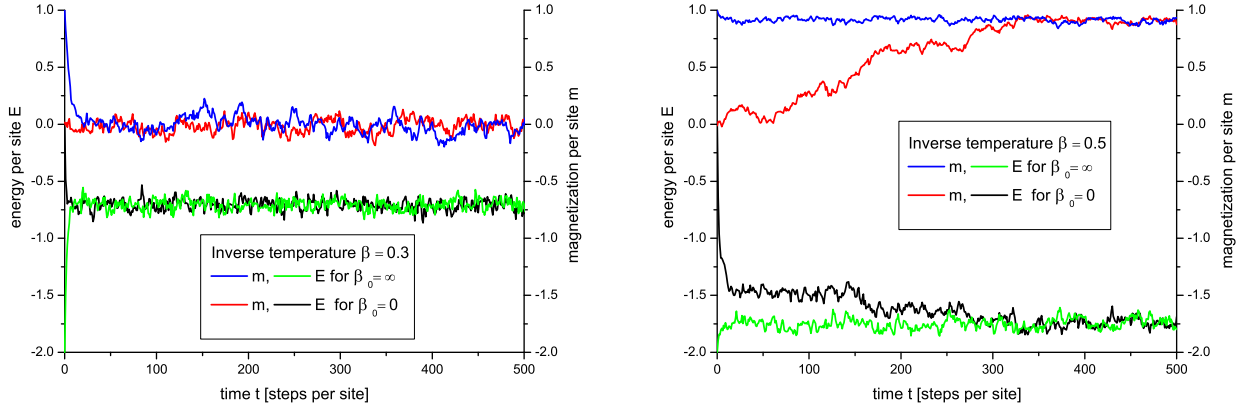


Figure 1: Thermalization processes of  $m$  and  $E$  outside the critical region.

Figure 1 shows the thermalization process of the magnetization  $m$  and the energy  $E$  for  $\beta = 0.3$  and  $\beta = 0.5$ , respectively, constituting the borders of the interval we are interested in. Such measurements were performed for different values of  $\beta$  in this interval. Since measurements with different initial states stabilize at the same values, one can conclude that indeed an equilibrium is reached. Furthermore, it is apparent that the thermalization time increases with  $\beta$  and that an equilibrium is reached much faster when starting from a polarized state.

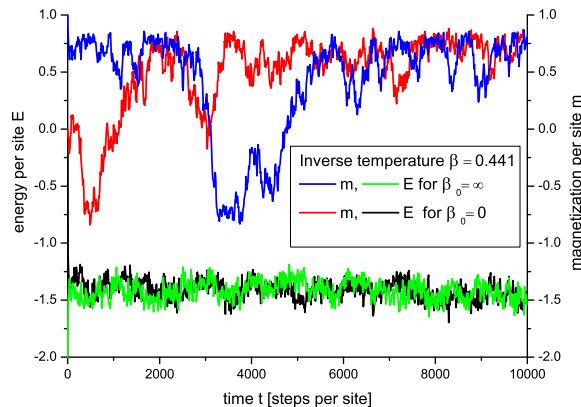


Figure 2: Thermalization process at  $\beta_c$ . The scale on the  $x$ -axis is 10 times longer than in Figure 1.

In the “critical region” close to the theoretical value of the critical inverse temperature,  $\beta_C \approx 0.441$ , the situation changes drastically as shown in Figure 2. In particular, the magnetization fluctuates heavily and it is not easy to determine when an equilibrium is reached. This phenomenon is known as “critical fluctuations”. It is pointed out that the time axis in Figure 2 is twenty times longer than in Figure 1. As the further measurements have to be performed on equilibrated data, the results of this section are carefully taken into account in the next sections.

## 2.2 Autocorrelation functions

A typical feature of Monte-Carlo methods is that a large number of samples is necessary to obtain accurate results. The correlations between samples should be as small as possible. Therefore, the autocorrelation time has to be calculated before performing any further measurements. When dealing with discrete measurements over a bounded time interval, the exact autocorrelation function cannot be determined. For a discrete variable  $X_k$  containing  $N$  measurements labeled by  $k = 0 \dots N - 1$ , the following discrete version is used instead

$$c(k) = \frac{1}{N-k} \sum_{i=0}^{N-k-1} X_{i+k} \left( X_i - \frac{1}{N-k} \sum_{i=0}^{N-k-1} X_j \right)$$

where the measurements have to be equally spaced in time, such that  $t = k\Delta t$ . These functions were determined for the energy  $E$  and the absolute value of the magnetization  $|m|$  at different values of the inverse temperature  $\beta = 0.3 \dots 0.5$  in steps of 0.01.

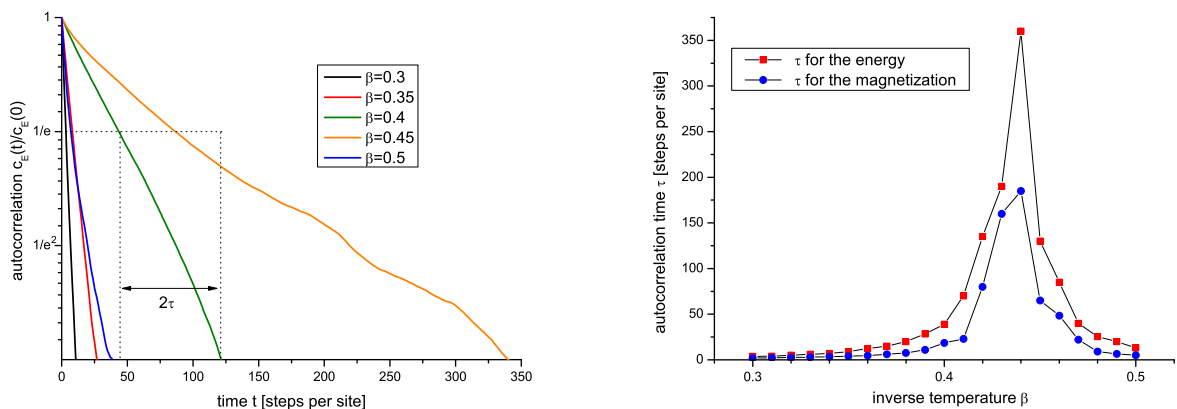


Figure 3: Left: Some autocorrelation functions for  $E$  for different values of  $\beta$ . For each curve an average was taken over 10 measurements, each consisting of  $2 \cdot 10^4$  samples taken after equilibration. Right: Autocorrelation times for  $E$  and  $m$  as a function of  $\beta$ .

The left graph in Figure 3 shows several measurements of the autocorrelation function for the energy normalized to  $c_E(0) = 1$  on a logarithmic scale. In the range below  $1/e^3$  not depicted here, the data gets more and more noisy. Analogous curves were found corresponding to  $m$ . Since the data behaves approximately linear at least within a certain range, the autocorrelation may be approximated through  $\frac{c(t)}{c(0)} \approx e^{-\frac{t}{\tau}}$ . The autocorrelation time  $\tau$  (in steps per lattice site) is then found from the inverse function of the autocorrelation function via

$$(n-1)\tau = c^{-1}(e^{-n}) - c^{-1}(e^{-1}).$$

The result is shown in the right graph in Figure 3. The autocorrelation times reach a maximal value around  $\beta_c$  (“critical slowing down”) and rapidly decrease outside that area. The values obtained for the two functions are within the same order of magnitude. In order to obtain proper results, all further measurements maintain a period of at least  $3\tau$  between two consecutive samples taken.

An interesting theoretical property of the autocorrelation time gives a reason for the limitations of the Metropolis algorithm when it comes to larger lattices. It can be shown that  $\tau \propto L^z$  in the critical region, where  $z \approx 2.2$  is the dynamic exponent for this algorithm. Since the number of single Monte-Carlo steps forming one step per site is  $L^2$ , the computation time can be estimated to scale *at least* with  $L^4$ , so that computations slow down significantly for larger  $L$ .

## 2.3 Magnetization and magnetic susceptibility

Armed with the results of the previous sections, the measurements for the absolute value of the magnetization  $|m|$  and the susceptibility  $\chi$  are performed. Starting from a fully polarized state,  $\beta$  is successively lowered from 0.5 to 0.3, where the step size is 0.01 outside the critical region and 0.005 inside. For every value of  $\beta$ ,  $10^4$  samples are taken after equilibration. The samples are separated by at least  $3\tau$ .

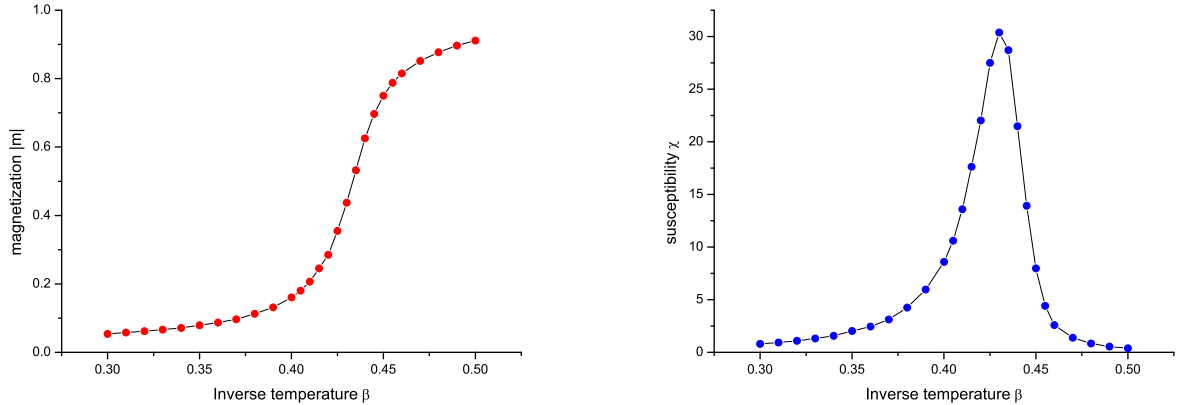


Figure 4: Magnetization  $|m|$  per site and susceptibility  $\chi$  as a function of  $\beta$  for  $L = 40$ , computed with the Metropolis algorithm. Each point corresponds to  $10^4$  samples.

The computation lasted several hours, and the results are shown in Figure 4. Clearly, *signs* of a phase transition can be seen, since the magnetization increases rapidly in a region around  $\beta_C \approx 0.441$ . However, a finite-size system is considered here and the behaviour indeed differs from what the theory predicts for the thermodynamic limit. The magnetization does not drop to zero for  $\beta < \beta_C$ , and the susceptibility only reaches a maximum, but does not diverge. The location of this maximum cannot simply be associated with  $\beta_C$ , what will become apparent in the next chapter.

## 3 The Wolff algorithm

The Metropolis algorithm considered in the previous chapter is easy to implement, but also quite slow. In particular, it can take considerable time at low temperatures until a cluster of spins directed opposite to the prevailing direction is flipped. This is because the Metropolis algorithm acts locally and does not know about these clusters.

A faster alternative are cluster flipping algorithms, such as the Wolff algorithm considered in this chapter. Starting from a randomly chosen “seed” of a cluster  $C$ , this algorithm looks at all neighboring links  $\langle x, y \rangle$  with  $x \in C$  and  $y \notin C$ . The probability of adding this link to the cluster that is to be flipped is set to

$$P_{act} = \begin{cases} 0 & \text{if } \sigma_x \neq \sigma_y \\ 1 - e^{-2\beta J} & \text{if } \sigma_x = \sigma_y \end{cases}$$

in order to obtain detailed balance. The implementation used here is based on a FIFO-buffer.

### 3.1 Magnetization and magnetic susceptibility

Using the Wolff algorithm, measurements of the magnetization  $|m|$  and the susceptibility  $\chi$  were performed in the same manner as in Section 2.3, but now for different lattice sizes  $L \in \{20, 30, 40, 50, 60, 100\}$ . In Figure 5, some of these measurements that best illustrate the characteristic changes with  $L$  were plotted. Of course, the curves for  $L = 40$  precisely coincide with the ones in Figure 4 as expected.

The graph on the left clearly shows that the progression of  $|m|$  becomes more and more similar to the curve expected for an order parameter of a second order phase transition as  $L$  grows. As it can

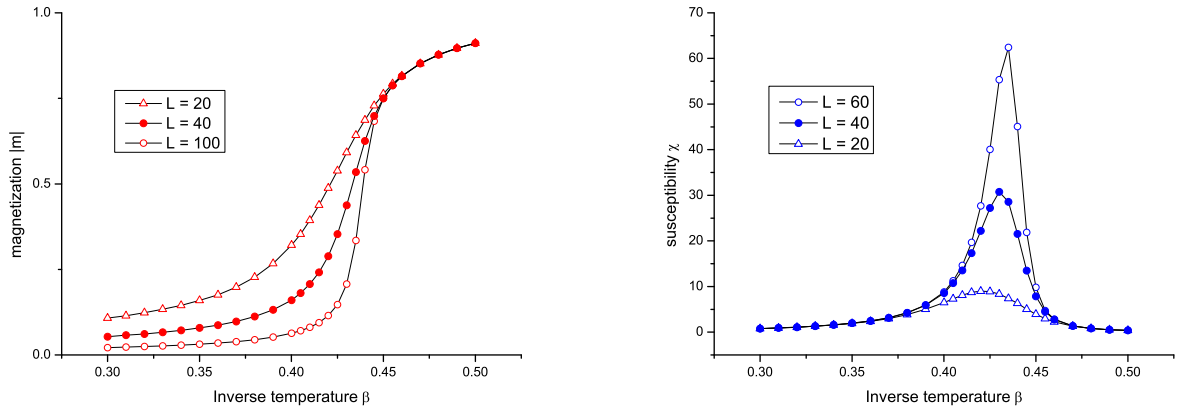


Figure 5: Magnetization  $|m|$  per site and susceptibility  $\chi$  as a function of  $\beta$  for some different lattice sizes, computed with the Wolff algorithm. Now, each point corresponds to  $10^5$  samples.

be seen in the graph on the right, the maximum of the susceptibility gets increasingly pronounced and approaches  $\beta_C$  with  $L$  becoming larger.

### 3.2 Data collapse for different lattice sizes

The whole set of data obtained in the previous section can now be evaluated using finite-size scaling. In an infinite-size system, many quantities diverge around the critical point. For example, in theory, the correlation length  $\xi$  and the susceptibility  $\chi$  diverge like

$$\xi \propto |t|^{-\nu} \quad \text{and} \quad \chi \propto |t|^{-\gamma}$$

where  $\nu$  and  $\gamma$  are the critical exponents, if the reduced temperature  $t = \frac{T-T_C}{T_C}$  approaches zero. But on a finite lattice,  $\chi$  cannot become larger than  $L$  and it can be derived that

$$\chi = L^{\frac{\gamma}{\nu}} \tilde{\chi}(L^{1/\nu} t)$$

where  $\tilde{\chi}$  is the *scaling function* which is independent of  $L$ . Thus, by plotting  $\tilde{\chi} = L^{-\gamma/\nu} \chi$  as a function of  $L^{1/\nu} t$ , the curves for different values of  $L$  should coincide at least near the critical region for an appropriate choice of  $T_C$ ,  $\gamma$  and  $\nu$ .

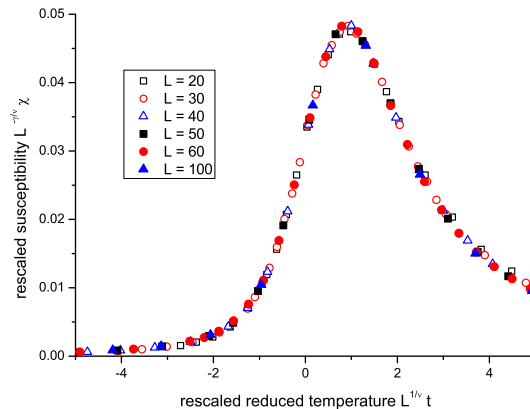


Figure 6: The scaling functions  $\tilde{\chi}$  for six different lattice sizes, with  $\gamma = 1.75$ ,  $\nu = 1$  and  $T_C = 2.27$

Figure 6 illustrates the results of this analysis. Trying to make the curves overlap simply by visual judgement, it turns out that the curves match best when choosing  $\gamma = 1.75 \pm 0.02$ ,  $\nu = 1 \pm 0.02$  and  $T_C = 2.27 \pm 0.01$ . These values are in accordance with the theoretical values  $\gamma = \frac{7}{4}$ ,  $\nu = 1$  and  $T_C = 2.269$ . Evidently, the maximum of  $\tilde{\chi}$  is quite close to 1. Hence, the shift of the maximum of the susceptibility for a lattice with a side length of  $L$  can be roughly estimated by

$$\beta_{\max,L} \approx \beta_C \frac{L}{L+1}$$

where the exact value  $\nu = 1$  is used. This again illustrates the shift shown on the right-hand side in Figure 5.

## 4 Conclusions

The simulations of the 2-dimensional Ising model with the Metropolis algorithm and the Wolff algorithm verify that this model shows a second-order phase transition with  $|m|$  as order parameter. The Metropolis algorithm is easier to implement, but the Wolff algorithm is much more efficient. It allows to increase the lattice size and to obtain more accurate results at the same time. The method of finite-size scaling offers an elegant way both to compare data from differently sized lattices and to determine the relevant parameters  $\gamma$ ,  $\nu$  and  $T_C$ . These turn out to be in line with the analytical solution.

The accuracy of the results could be further improved by using larger lattices and taking more samples. However, to keep the computation times reasonably short, more elaborate techniques, such as parallel computing or multi-spin coding, would be necessary.

## References

- [1] M. E. J. Newman and G. T. Barkema. *Monte Carlo Methods in Statistical Physics*. Oxford University Press, 1999.
- [2] F. Schwabl. *Statistical Mechanics*. Springer, 2006.